Published in final edited form as:
Dev Cell. 2012 October 16; 23(4): 716–728. doi:10.1016/j.devcel.2012.08.010.

kinesin-13 and tubulin post-translational modifications regulate microtubule growth in axon regeneration

Anindya Ghosh-Roy[1], **Alexandr Goncharov**[1,2], **Yishi Jin**[1,2], and **Andrew D. Chisholm**[1]

[1]Division of Biological Sciences, Section of Neurobiology, University of California San Diego, 9500 Gilman Drive, La Jolla, CA 92093

[2]Howard Hughes Medical Institute

Summary

The microtubule (MT) cytoskeleton of a mature axon is maintained in a stabilized steady state, yet after axonal injury can be transformed into a dynamic structure capable of supporting axon regrowth. Using *C. elegans* mechanosensory axons and in vivo imaging we find that in mature axons the growth of MTs is restricted in the steady state by the depolymerizing kinesin-13 family member KLP-7. After axon injury, we observe a two-phase process of MT growth upregulation. First, the number of growing MTs increases at the injury site, concomitant with local downregulation of KLP-7. A second phase of persistent MT growth requires the cytosolic carboxypeptidase CCPP-6, which promotes Δ2 modification of α-tubulin. Both phases of MT growth are coordinated by the DLK-1 MAP kinase cascade. Our results define how the stable MT cytoskeleton of a mature neuron is converted into the dynamically growing MT cytoskeleton of a regrowing axon.

Keywords

C. elegans; microtubule dynamics; DLK-1 MAP kinase; depolymerizing kinesin; tubulin tyrosine ligase; cytosolic carboxypeptidase; Δ2-tubulin

Introduction

Microtubules (MTs) define and maintain neuronal polarity, and act as highways for transport of proteins and organelles to cell compartments distant from the neuronal cell body (Witte and Bradke, 2008). MTs are intrinsically unstable, exhibiting dynamic instability in vitro (Mitchison and Kirschner, 1984) and in vivo (Cassimeris et al., 1988). Dynamic instability is a hallmark of MTs in cells or compartments that undergo rapid morphological changes, such as dividing cells or axonal growth cones (Suter et al., 2004). In contrast, long-lived cellular compartments such as axons or dendrites are enriched in stabilized MTs (Baas et al., 1993). In early neuronal development MT stabilization plays an instructive role in selection of a single neurite as the future axon (Witte et al., 2008). Subsequently, dynamic MTs are spatially and temporally regulated such that they are confined to growth cones or sites of branch formation (Yu et al., 1994). Finally, the integrity of mature neurons in a functional

Correspondence to: Andrew D. Chisholm.

circuit requires a stabilized axonal and dendritic MT cytoskeleton, although such neurons retain latent plasticity in their MT arrays (Bradke and Dotti, 2000; Gomis-Ruth et al., 2008).

The MT cytoskeleton of mature axons is composed of two types of MT, stable and labile (Ahmad et al., 1993). Neurons are rich in microtubule-associated proteins that stabilize the axonal MT array, including tau, MAP1B, and STOP (Dehmelt et al., 2003; Guillaud et al., 1998). Such factors counteract the effects of MT-severing enzymes such as spastin or katanin(Baas and Qiang, 2005). Recent work has also revealed the critical roles of tubulin post-translational modifications in regulating MT stability (Janke and Kneussel, 2010). α-tubulins are deglutamylated at their C-termini by cytosolic carboxypeptidases or CCPs (Rogowski et al., 2010). α-tubulins lacking C-terminal tyrosine and glutamate, also known as Δ2-tubulin, form extremely stable microtubules (Paturle-Lafanechere et al., 1994). Lack of the CCP Nna1 leads to late-onset neuronal degeneration (Fernandez-Gonzalez et al., 2002), suggesting that stable MTs maintain axonal integrity. Detyrosination, but not Δ2 formation, can be reversed by tubulin tyrosine ligases (TTLs); MTs enriched in tyrosinated α-tubulin are less stable as they are more sensitive to MT depolymerizing enzymes such as the kinesin-13 family member MCAK (Peris et al., 2009). At present, little is known about how such MT regulatory factors are regulated in mature neurons.

Mature axons are frequently capable of remarkable regenerative growth after injury(Ramon y Cajal, 1928). Such regrowth often involves the regeneration of a severed axon stump into a motile growth cone resembling those of developmental outgrowth(Bradke et al., 2012). The ability of axons to regenerate after injury must therefore involve local conversion of a stable MT cytoskeleton into the growing MT cytoskeleton of a motile growth cone(Erez and Spira, 2008). Indeed an early axonal response to injury is the local disassembly or severing of axonal MTs, potentially creating free plus ends that allow new MT polymerization. Conversely, moderate stabilization of axonal MTs by Taxol can promote axon regrowth in the inhibitory microenvironment of the mammalian CNS (Hellal et al., 2011; Sengottuvel et al., 2011). Drugs that promote MT growth can also promote axon regeneration on inhibitory substrates in vitro (Usher et al., 2010). Once new dynamic MTs have been generated, they must undergo persistent growth to permit axon elongation. However the mechanisms by which the MT cytoskeleton is remodeled after injury are unclear. A better understanding of MT remodeling mechanisms will provide insights into the initial stages of axon regrowth.

C. elegans is a tractable model for studies of axon regrowth after injury (Chen and Chisholm, 2011; Gabel et al., 2008; Samara et al., 2010; Wu et al., 2007). Many *C. elegans* axons can regrow after laser axotomy, which triggers second messenger cascades related to those involved in regrowth in other organisms (Ghosh-Roy et al., 2010). Genetic screens have identified many genes and pathways specifically required for adult axon regrowth (Chen et al., 2011)(Bejjani and Hammarlund, 2012). Among these, the DLK-1 MAPK cascade is essential for early stages of regrowth (Hammarlund et al., 2009; Yan et al., 2009), a function conserved in insects (Xiong et al., 2010) and in mammals (Itoh et al., 2009)(Shin et al., 2012). One effector of the DLK-1 pathway in *C. elegans* is the bZip protein CEBP-1(Yan et al., 2009), but the DLK-1 pathway likely has additional targets. A second MAPK cascade, the MLK-1/KGB pathway, acts in parallel to the DLK pathway in regrowth (Nix et al., 2011).

Here, using in vivo live imaging in *C. elegans* axons, we show that mature axons contain a small population of growing MTs that are maintained in an unstable state by KLP-7, a member of the kinesin-13 family of MT-depolymerizing kinesins. Axonal injury triggers local downregulation of KLP-7 and upregulation of growing MTs at the injured axon tip. MTs then enter a second phase of persistent growth, dependent on cytosolic carboxypeptidases that promote the Δ2 post-translational modification of tubulin. We show

that the DLK-1 pathway promotes both MT upregulation and growth persistency. Our results elucidate the mechanisms that convert the stable MT axon cytoskeleton into a dynamically growing state.

Results

Two phases of MT growth regulation are triggered by axon injury

To visualize the effects of axotomy on microtubules in vivo, we used GFP-tagged MT plus-end binding proteins (EBP-1, EBP-2), established markers of the plus ends of growing MTs in neurons (Stepanova et al., 2003). We expressed EBP-1::GFP or EBP-2::GFP in PLM touch neurons, and imaged them in immobilized animals using spinning disc confocal microscopy (Figure 1A, Figure S1A). We divided touch neuron axons into adjacent 40 μm regions of interest (ROIs) to define the local behavior of MTs (Figure 1A). For each ROI we imaged EBP-2::GFP dynamics (Experimental Procedures; Supplemental Movie 1) and analyzed the results in kymographs (Figure 1B). We observed similar patterns using EBP-1::GFP (Figure S1A–C), and refer collectively to these markers as EBP-GFP. We quantitated total numbers of EBP-GFP 'comets' (tracks in kymographs) as well as their growth duration, length, and velocity. In the steady state, EBP-GFP comets were most abundant in or close to the PLM soma; axons contained comparatively few comets that grew for short periods (5.9 ± 0.2 s in ROI-A; red arrow, Figure 1A–C). More distal axon regions also had few growing MTs that underwent frequent catastrophe (not shown). Almost all EBP-GFP comets grew away from the cell body, suggesting that MT polarity in the PLM process is plus-end-out, exhibiting axonal rather than dendritic MT polarity. EBP-GFP based assays do not detect stable MTs, but based on EM studies the PLM axon typically contains 20–50 MTs at any one position (Chalfie and Thomson, 1979); see also Figure S1. The steady-state pool of growing MTs is therefore small compared to the stable MT pool. Although MTs are particularly abundant in touch neurons, the EBP-GFP dynamics parameters reported here appear similar to those observed in other *C. elegans* neurons (Goodwin et al., 2012; Hao et al., 2011; Maniar et al., 2012). EBP-GFP dynamics parameters reported here are summarized in Table S1.

To address how axonal injury affected MT dynamics we severed PLM axons 100 μm from the cell body by laser microsurgery (see Experimental Procedures; Figure 1D′). At 3 h after axotomy the number of EBP-GFP tracks increased over three-fold near the cut site (ROI-A, purple traces, Figure 1D,E; Supplemental Movie 2) compared to uninjured axons (2.9 ± 0.2 at 0 h vs. 10.3 ± 1.1 at 3 h). At times before 3 h this upregulation was not statistically significant (not shown). The length and duration of EBP-GFP tracks at 3 h was not significantly different from that in uninjured axons. The number of EBP-GFP tracks continued to rise at later time points, although the increase was most significant from 0–3 h (Figure 1E). Further away from the injury site (ROI-B) the number of EBP-GFP tracks remained low (Figure 1E). We found similar local upregulation of growing MTs after axotomy at 60 μm from the cell body, the position used in our standard axon regrowth assay (Figure S1D,E). In summary, an early response to injury of the PLM axon is a local upregulation of growing MTs close to the axon stump.

EBP-GFP comets at the severed axon tip at 3 h had a similar catastrophe frequency (Figure 1F) as comets in uninjured axons. Between 3 and 6 h, EBP-GFP tracks in ROI-A decreased over two-fold in catastrophe frequency (Cassimeris et al., 1988) and doubled in length (Figure 1F,G), indicating an increase in persistent MT growth. The number and length of EBP-GFP tracks did not significantly change away from the axon tip (in ROI-B, Figure 1E; length data not shown). Injured PLM axons form a growth cone-like structure and begin extending by 4.5–6 h after injury (Wu et al., 2007). The transition to more persistent MT growth therefore correlates with reformation of a growth cone and the beginning of axon

extension. The number and length of EBP-GFP comets continued to increase; a notable change at 10.5 h was a significant increase in EBP-GFP comet growth velocity (Figure 1H). With this analysis of the normal response to injury in hand, we investigated which regulators of MT dynamics affect axon MT remodeling.

The kinesin-13 KLP-7 maintains steady-state growing microtubules and inhibits MT upregulation in early regrowth

Proteins that induce MT depolymerization, known as 'catastrophe factors', are central regulators of MT dynamics. As *C. elegans* lacks orthologs of catastrophe factors such as stathmins (Cassimeris, 2002), we focused on the conserved kinesin-13 family of depolymerizing kinesins (Howard and Hyman, 2007). Kinesin-13 family members such as KIF2B or KIF2C/MCAK diffuse along the MT lattice until they reach plus-ends, where they depolymerize the stable GTP-containing cap of a growing MT (Helenius et al., 2006). All kinesin-13s tested display similar catastrophe-inducing activity in vitro, and studies of the *C.elegans* kinesin-13, KLP-7, in the early embryo are consistent with it acting as a MT catastrophe factor (Srayko et al., 2005). *klp-7(tm2143)* null mutants, denoted *klp-7(lf)* (Figure S2A), display incompletely penetrant maternal-effect lethality, but grow to adulthood at normal rates, allowing analysis of the role of KLP-7 in neurons. In *klp-7(lf)* mutants PLM and ALM frequently extended ectopic neurites from their cell bodies; ALM often had a bipolar morphology (Figure S2B,C). These phenotypes were rescued by transgenes containing *klp-7(+)* genomic DNA or expressing KLP-7 under the control of the *unc-86* promoter, expressed early in the touch cell lineage(Finney and Ruvkun, 1990) (Figure S2B), but not by expression from the *mec-4* promoter, active in differentiated touch neurons (Duggan et al., 1998). KLP-7 may therefore act early in development to ensure that touch neurons extend a single axon. In mature PLM neurons, *klp-7(lf)* mutants displayed almost no EBP-GFP comets (Figure S2D; Supplemental Movie 3). Moreover, by EM analysis, *klp*-7 axons contained ~50% as many MTs as the wild type (Figure S1), suggesting KLP-7-dependent catastrophe maintains steady state MT number. However, overexpression of KLP-7 did not increase the number of EBP-GFP comets in the steady state (Figure 2A), consistent with most steady state MTs being insensitive to KLP-7 activity.

Despite the lack of EBP-GFP comets in uninjured *klp-7(lf)* axons, axotomy triggered a robust local increase in EBP-GFP comets (Figure 2A; Supplemental Movie 4). EBP-GFP comet lengths (Figure 2B) and duration (not shown) were significantly increased in *klp-7(lf)* at 3 h compared to wild type, suggesting that in the wild type, KLP-7 maintains the newly upregulated MTs in an unstable state. As regrowing axons in *klp-7(lf)* animals typically extended into multiple focal planes by 6 h we were unable to quantitatively image EBP-GFP dynamics at later time points; in rare cases where we could image the axon tip at 6 h, EBP-GFP tracks underwent more persistent growth compared to wild type (Figure S2D). *klp-7* was not recovered in large-scale screens for regrowth mutants (Chen et al., 2011), as *klp-7(lf)* mutants do not dramatically affect regrowth at the 24 h time point (Figure 2E). However *klp-7(lf)* mutants displayed significantly increased regrowth at early time points (4.5 h; Figure 2C). Thus, initial axon regrowth correlates with increased MT growth persistence rather than absolute number of growing MTs. Conversely, overexpression of KLP-7 in touch neurons (P*mec-4*-KLP-7) blocked the axotomy-induced up-regulation in growing MTs (Figure 2A), and reduced MT growth at 6 h post-axotomy (Figure 2B). After axotomy, KLP-7-overexpressing axons formed large growth cone-like structures that failed to extend (arrowhead, Figure 2F), leading to strongly reduced regrowth at 24 h. We conclude that KLP-7 inhibits up-regulation of growing MTs and their subsequent growth.

KLP-7, like other kinesin-13s, consists of a central motor domain flanked by N-terminal and C-terminal domains (Desai et al., 1999) (Figure 2D). The region between the N-terminus and the motor domain is termed the neck (Vale and Fletterick, 1997). Deletion of either the

N-terminal domain or of the neck reduces the ability of MCAK to depolymerize MTs (Ems-McClung et al., 2007; Maney et al., 2001; Montenegro Gouveia et al., 2010). By expressing deletion constructs of KLP-7 in touch neurons we found that aa 58-149 of KLP-7 were critical for its ability to inhibit axon regrowth (Figure 2E). This region contains a tetrapeptide SMIL (Figure S2E) that resembles the SxIP motif shown in other proteins to mediate interaction with EB1 (Honnappa et al., 2009). Mutation of SMIL to SMNN in full-length KLP-7 abolished its growth-inhibiting activity (Figure 2E). Expression of the KLP-7 N-terminus alone (aa 1-240) did not inhibit regrowth (Figure 2E), implying that effects of KLP-7 overexpression do not reflect titration of end-binding proteins, and that the KLP-7 motor domain is also important. Thus the regrowth-inhibiting effects of KLP-7 likely require targeting to MT plus ends.

In summary, KLP-7 maintains a low number of growing axonal MTs in the steady state, and inhibits axotomy-triggered upregulation of MTs. In the absence of KLP-7, initiation of axon regrowth is accelerated, but long-term axon extension is not enhanced, suggesting that other factors protect axon MTs from KLP-7 activity during later stages of regeneration.

Axon regeneration is influenced by tubulin post-translational modifications

Screens for genes affecting PLM axon regeneration have revealed roles for MT-associated proteins including the plus-end binding protein EBP-1 (Chen et al 2011). To identify other pathways that could mediate the effects of axotomy on axonal MT dynamics, we conducted a more in-depth screen of MT dynamics regulators (Figure S3A) and identified important roles for tubulin post-translational modifications in axon regrowth.

MT post-translational modification enzymes fall into two classes: ligase-like enzymes that add modifications (tyrosination, polyglutamylation, acetylation), and carboxypeptidases that remove modifications. We focused on the tubulin tyrosine ligase-like (TTLL) enzymes, of which *C. elegans* encodes six (Kimura et al., 2010), and on the cytosolic carboxypeptidases CCPP-1 and CCPP-6 (O'Hagan et al., 2011). Although lack of CCPs can result in degeneration of neuronal processes(Rogowski et al., 2010) or aberrant ciliated endings(O'Hagan et al., 2011), touch neuron morphology appeared normal in *ccpp* mutants (not shown). PLM regrowth was significantly impaired in *ccpp-6* mutants, and to a lesser extent in *ccpp-1* mutants (Figure 3A,B); *ccpp-1 ccpp-6* double mutants resembled *ccpp-6*. Expression of CCPP-6 in touch neurons fully rescued the *ccpp-6* regrowth phenotype (Figure 3A,B), indicating CCPP-6 acts cell autonomously. Out of several *ttll* genes tested, only *ttll-5(lf)* mutants displayed enhanced axon regrowth (Figure 3B, S3A). As TTLL-5 catalyzes polyglutamylation (Kimura et al., 2010), tubulin polyglutamylation may inhibit axon regrowth. *ttll-9(lf)* mutants did not display dramatic effects on regrowth at 24 h but showed highly penetrant developmental overgrowth of PLM (Figure S3B,C), reminiscent of the neurite overgrowth in mouse TTL mutants (Erck et al., 2005).

We next tested whether tubulin-modifying enzymes affected regrowth via altered axonal MT dynamics. In *ccpp-6* and *ttll-5* mutants the total number of EBP-GFP comets was normal both before and after axotomy (Figure 3C,D). Instead, these mutants displayed specific and opposing effects on MT growth. In *ccpp-6* mutants the length and duration of EBP-GFP tracks were significantly reduced at 6 h (Figure 3C,E), suggesting that in the absence of CCPP-6, MTs are unable to convert to stabilized growth. Conversely, in *ttll-5* mutants, EBP-GFP track duration significantly increased at 3 h post axotomy compared to wild type, suggesting an accelerated transition to persistent growth. At 6 h post axotomy, *ccpp-6* mutants displayed decreased PLM regrowth and fewer growth cones, whereas *ttll* mutants showed increased growth cone formation (Figure S3D), indicating that in some mutant backgrounds regrowth at 24 h correlates with initial growth cone formation.

Loss of CCPP-6 function inhibits injury-triggered MT growth and impairs axon regrowth. We reasoned that the inability of *ccpp-6* mutants to promote MT growth might reflect elevated sensitivity of polyglutamylated MTs to the depolymerizing activity of KLP-7. Consistent with this hypothesis, *klp-7(lf)* completely suppressed the regeneration defects of *ccpp-6* mutants (Figure 3A,B). As shown below (Figure 6), *ccpp* and *ttll* mutants have the expected effects on tubulin post-translational modification levels. Taken together, PLM regrowth is promoted by CCPP-dependent modifications, and inhibited by TTLL-dependent modifications.

The DLK-1 MAPK cascade regulates axonal MT dynamics

The potent effects of KLP-7 and MT post-translational modification enzymes on regrowth suggested that these factors are tightly regulated during regenerative growth. To address mechanisms of regulation we focused on the DLK-1 MAP kinase cascade, which is essential for axon regrowth (Hammarlund et al., 2009; Yan et al., 2009) and which has been proposed to influence MT dynamics in vertebrate neurons (Hirai et al., 2011; Lewcock et al., 2007). *dlk-1* loss of function blocks axon regrowth, whereas DLK-1 overexpression enhances regrowth (Hammarlund et al., 2009; Yan et al., 2009). We first asked whether loss or gain of function in DLK-1 affected axonal MT dynamics. *dlk-1(lf)* mutants displayed normal EBP-GFP comets in the steady state (Figure 4A,B) and normal numbers of PLM MTs by EM (Figure S1). The initial upregulation of growing MTs after axotomy was reduced, although not eliminated (1.6-fold upregulation, $P = 0.14$; Figure 4A,B). However, MTs failed to switch to persistent growth by 6 h in *dlk-1(lf)* mutants (Figure 4A,C). Conversely, DLK-1 overexpression had dramatic effects on growing MTs, causing a 4-fold increase in the number of EBP-GFP comets (12.8 ± 1.9 in DLK-1[++] vs. 2.9 ± 0.2 in wild type, Figure 4A,B), both before and after axotomy. In DLK-1[++] axons, MTs underwent a premature transition to persistent growth at 3 h after axotomy (Figure 4A,C). Thus, DLK-1 is not essential for growing MTs in the steady state, consistent with low levels of DLK-1 pathway activity in uninjured neurons(Nakata et al., 2005).

We next asked whether the effects of DLK-1 on MT number and dynamics involved its major known target, the bZip protein CEBP-1 (Yan et al., 2009). EBP-GFP dynamics before and after axotomy appeared largely normal in *cebp-1(lf)* mutants; the only detectable phenotype in *cebp-1(lf)* mutants was a reduction in EBP-GFP growth velocity at 6 h post injury (Figure S4). We infer that the failure of *dlk-1(lf)* mutants to form persistently growing axonal MTs is not a consequence of a block in regeneration, and that the roles of the DLK-1 pathway in MT growth control are largely independent of CEBP-1.

Negative regulation of KLP-7 can partly bypass the requirement for DLK-1 in regrowth

As DLK-1 promotes upregulation of MTs after injury (Figure 4) we asked whether the DLK-1 pathway might counteract the effects of KLP-7. *klp-7(lf)* significantly suppressed the regeneration defects of *dlk-1(lf)* mutants and of the DLK-1 downstream p38/MAPK *pmk-3* (Figure 5A), consistent with the DLK-1 kinase cascade inhibiting KLP-7. *klp-7(lf)* also significantly suppressed the regrowth defects of *kgb-1* mutants (Figure 5A), suggesting loss of KLP-7 does not simply upregulate the parallel KGB MAPK pathway. Loss of KLP-7 function also suppressed the *pmk-3* regrowth defect in GABAergic motor neurons (Figure 5B), indicating that KLP-7 restrains regrowth of multiple neuron types.

To address how the DLK-1 pathway might negatively regulate KLP-7 in regrowth we examined KLP-7 localization. GFP::KLP-7 puncta were distributed along axons; they displayed local motility but did not undergo long-range movement (Supplemental Movie 5; Figure S6C), consistent with *in vitro* studies of kinesin-13 (Helenius et al., 2006). After axotomy, GFP::KLP-7 intensity became significantly reduced in the axon close to the cut

site (Figure 5C,D). In contrast, cytosolic GFP (not shown) or EBP-2::GFP intensities were unaffected after axotomy (Figure S1F,G), indicating that the severed end does not simply shrink or disassemble the MT cytoskeleton. In *dlk-1(lf)* mutants GFP::KLP-7 levels were normal prior to axotomy (Figure S6A,B) and remained unchanged after axotomy (Figure 5C,D); in axons overexpressing DLK-1, GFP::KLP-7 was mostly retained in the soma (Figure 5E, S5A,B). These findings are consistent with the DLK-1 pathway negatively regulating KLP-7 localization to axons by reducing KLP-7's affinity for axonal MTs.

Phosphorylation of the N-terminus or neck of kinesin-13s reduces their affinity for MTs, inhibiting their MT-depolymerizing activity(Andrews et al., 2004; Lan et al., 2004; Zhang et al., 2007). By analogy, the DLK-1 pathway could reduce the MT binding affinity of KLP-7 by phosphorylation, allowing KLP-7 to be excluded from the injured axon tip. We therefore screened the KLP-7 N-terminus for potential sites of regulation (Figure 2D; Supplemental Experimental Procedures). As wild type KLP-7 inhibits regeneration we hypothesized that phosphomimetic mutants in KLP-7 would not be able to inhibit regeneration. Among several constructs, only phosphomimetic mutations in the N1 region abrogated the growth-inhibiting activity of KLP-7 (Figure 2E). Conversely, non-phosphorylatable mutations in the N1 domain (N1S-A) blocked the local removal of GFP::KLP-7 from the axon tip (Figure 5D). The N1 region contains the SMIL motif, whose ability to interact with EB1 can be negatively regulated by phosphorylation of nearby residues (Honnappa et al., 2009). Overall, our analysis is consistent with the DLK-1 pathway regulating KLP-7 via phosphorylation, thereby locally inhibiting KLP-7 MT binding and depolymerization activity at the axon tip.

The DLK-1 pathway promotes formation of stable Δ2-modified tubulin

The partial suppression of *dlk-1(lf)* by *klp-7(lf)* suggested that the DLK-1 pathway might have other outputs in controlling the axon MT cytoskeleton. As *dlk-1(lf)* and *ccpp-6(lf)* had similar effects on axon MT growth after injury (Figures 3E,4C), we investigated whether the DLK-1 pathway might modulate tubulin post-translational modifications. We performed immunostaining using antibodies against conserved epitopes specific to the stable form Δ2-α-tubulin, to the less stable tyrosinated α-tubulin, and to pan-α-tubulin (see Experimental Procedures; staining quantitation is summarized in Table S2). CCPs promote formation of Δ2-tubulin (Rogowski et al., 2010), and as expected Δ2-tubulin immunostaining in PLM axons was strongly reduced in *ccpp-1(lf); ccpp-6(lf)* double mutants (Figure 6A,B). *dlk-1(lf)* mutants displayed significantly reduced levels of axonal anti-Δ2 immunostaining, whereas DLK-1 overexpression caused a significant increase in anti-Δ2 staining (Figure 6A,B). Conversely, levels of tyrosinated α-tubulin in PLM were elevated in *dlk-1(lf)* mutants (Figure 6C,D; Table S4), a phenotype rescued by neuronal expression of DLK-1. Levels of pan-α-tubulin in PLM were normal in *ccpp-1; 6* and in *dlk-1* mutants, consistent with our conclusions from EM that the number of axonal MTs is not altered in *dlk-1(lf)*. However pan-α-tubulin immunostaining levels were significantly increased in DLK-1 overexpressors (Figure 6B), suggesting that the MT-stabilizing effects DLK-1 overexpression may result in elevated levels of axonal tubulins. Anti-Δ2 and DM1A staining levels were normal in *cebp-1* and *klp-7* mutants (Table S2), indicating that the DLK pathway plays specific roles in tubulin modification.

The observed modulation of tubulin post-translational modifications by DLK-1 could be explained if the DLK-1 pathway activated CCPPs or inhibited TTLLs. Neuronal expression of a functional CCPP-6::GFP reporter was significantly reduced in *dlk-1(lf)* mutants (Figure S6), consistent with the DLK-1 pathway promoting CCPP-6 expression. Conversely, *dlk-1(lf)* mutants displayed enhanced neuronal expression of a TTLL-9::GFP reporter (Figure S6), suggesting the DLK pathway directly or indirectly represses TTLL-9 activity. We next addressed the functional relationship of DLK-1 and the tubulin modifying enzymes

in regeneration. DLK-1 overexpression promotes regeneration in many regrowth-defective backgrounds (Chen et al., 2011; Yan et al., 2009). DLK-1 overexpression was unable to overcome the requirement for either *ccpp-6* or *ccpp-1* in regeneration (Figure S7A,B), consistent with DLK-1 acting upstream of CCPPs in regrowth. Developmental axon overgrowth phenotypes caused by DLK-1 overexpression were also partly suppressed by *ccpp-6(lf)* (Figure S7C,D), consistent with CCPP-6 acting downstream of the DLK-1 pathway However, neither overexpression of CCPP-6 (Figure 7A), nor loss of *ttll-5* function (Figure S7E,F) improved regeneration in the *dlk-1(lf)* background. We reasoned that the inability of *dlk-1(lf)* mutants to locally downregulate KLP-7 activity after injury might negate any effects of manipulating tubulin modifications. We therefore overexpressed CCPP-6 in *dlk-1 klp-7* double mutants and found that the combination of CCPP-6 overexpression and loss of *klp-7* function synergistically improved regrowth to approximately 65% of the wild type level (Figure 7A,B). The combination of *klp-7(lf)* and CCPP-6 overexpression did not significantly enhance regrowth in a wild type background, suggesting these factors are only limiting in situations such as *dlk-1(lf)* where MT growth regulation is specifically impaired. Thus, most of the requirement for DLK-1 in regrowth can be bypassed by simultaneous manipulations that mimic the two phases of MT dynamics regulation: downregulation of the KLP-7 catastrophe factor and upregulation of CCPP-dependent modifications (Figure 7C).

Discussion

A major question in the cell biology of axon regeneration is to understand how the stable microtubule cytoskeleton of mature axons is converted to the dynamically growing MTs of regrowing axons. After injury the mechanisms that keep axonal MTs in a mature steady state act as barriers to the processes of MT that convert the axon stump into a new growth cone. By combining live imaging and genetics we have defined mechanisms regulating axonal MTs in the steady state and in regrowth. Our analysis suggests that axonal MTs undergo two temporally distinct phases of upregulation: an initial increase in the local number of growing MTs, and a later increase in MT growth persistence. As the total number of growing MTs and their growth duration are interrelated parameters, these two phases may not be completely distinct in terms of underlying mechanism. Nevertheless the two phases can be distinguished genetically; for example, CCPPs are required for the second phase but not for the first.

C. elegans mechanosensory axons contain distinctive 15-protofilament MTs (Chalfie and Thomson, 1979). Although the touch neurons are somewhat unusual in their MT cytoskeleton, our analysis suggests that the mechanisms defined here also apply to neurons with more typical MT arrays such as motor neurons. Our analysis indicates that most mechanosensory axonal MTs are stable, with a relatively small pool of growing MTs per axon. This pool of growing MTs is eliminated in *klp-7* mutants, suggesting KLP-7 maintains the pool of dynamic MTs. The plus ends of axonal MTs are enriched for tyrosinated tubulin (Ahmad et al., 1993), rendering them prone to MCAK mediated depolymerization (Peris et al., 2009). We propose that in the steady state DLK-1 activity is low and active KLP-7 depolymerizes any growing MTs (Figure 7C). DLK-1 is also required for transcriptional responses to depolymerized MTs in uninjured neurons (Bounoutas et al., 2011). This homeostatic mechanism could regulate the normal proportional growth of an axon, and could be under the control of pathways that couple axon outgrowth to synaptogenesis or activity.

A disorganized axonal MT cytoskeleton after injury has been linked to the inability of adult mammalian CNS axons to regenerate (Erturk et al., 2007). We find that an early response to axotomy is the local up-regulation of growing MTs and their subsequent persistent growth.

As KLP-7 inhibits MT growth in the steady state, it acts as a barrier for MT growth following injury, and we find that KLP-7 becomes locally removed from the injured axon tip. The DLK-1 cascade is required to initiate regrowth, and for local removal of KLP-7. DLK-1 is only partly required for the initial upregulation of growing MTs after axotomy; the DLK-1-independent increase in MTs could reflect other processes that lead to increased free plus ends, such as mechanical breakage or enzymatic severing of MTs (Erez and Spira, 2008). Phosphorylation of MCAK decreases its affinity for MTs during mitosis (Andrews et al., 2004), and our mutational analysis of KLP-7 is consistent with the N1 region of KLP-7 being a target of phosphorylation by the DLK-1 pathway after axotomy. Indeed, a nonphosphorylatable form of KLP-7 failed to be downregulated at the axon tip. Local activation of the DLK-1 pathway could phosphorylate KLP-7 so it can no longer bind to and depolymerize MTs.

As KLP-7 levels remain normal further away from the axon tip, other mechanisms likely protect MTs from KLP-7 induced depolymerization. Our genetic analysis indicates that loss of KLP-7 alone is insufficient to enhance regrowth at the 24 h time point. However loss of KLP-7 can enhance long-term regrowth in situations where MT upregulation or stability is limiting, such as *ccpp-6, dlk-1,* or *pmk-3* mutants. α-tubulin detyrosination protects MTs from depolymerization by MCAK (Peris et al., 2009). Detyrosination is catalyzed by tubulin carboxypeptidases, which convert MTs into the stable detyrosinated Δ2-tubulin form (Rogowski et al., 2010). We find that the carboxypeptidase CCPP-6 is required for regrowth, yet this requirement can be overcome by loss of function in KLP-7. As detyrosination only occurs on polymerized α-tubulin, we propose that new MTs formed after injury become detyrosinated by CCPP-6, protecting them against KLP-7 depolymerization and promoting persistent MT growth (Figure 7C).

We find that a key output of the DLK-1 pathway is to regulate MT dynamics and post-translational modifications. *dlk-1* mutants, like *ccpp* mutants, have reduced axonal Δ2-tubulin, fail to form persistently growing MTs after axotomy, and are unable to initiate axon regrowth. Conversely, DLK-1 overexpression elevates axonal Δ2-tubulin, increases the numbers of growing axonal MTs, and enhances axon regrowth. Several lines of evidence indicate that the DLK-1 pathway could promote CCPP activity. Interestingly, in mammals the CCP Nna1 is transcriptionally upregulated in motor neurons after axotomy (Harris et al., 2000). Although we have not yet observed upregulation of tubulin modifications or of enzyme expression after axotomy, it will be important to determine whether such factors are acutely regulated by the DLK pathway.

Our results indicate that the DLK-1 pathway promotes axon regrowth in at least two ways: by downregulating an MT catastrophe factor, and by promoting post-translational modifications that render MTs less prone to catastrophe. In vertebrate neurons, loss of PHR1, a negative regulator of DLK, causes axon overgrowth and abnormal growth of MTs (Hendricks and Jesuthasan, 2009; Lewcock et al., 2007). In these studies the net effect of the DLK pathway was interpreted as being to destabilize MTs (Lewcock et al., 2007). In contrast, studies of the DLK loss of function phenotype in mouse brain development have been more consistent with DLK activity having an MT stabilizing effect in axon formation(Hirai et al., 2011). Our analysis of MT dynamics in vivo indicates that the DLK pathway overall promotes growth of axonal MTs. Our conclusions can be reconciled with those of previous studies if endogenous levels of DLK activity lead to an intermediate level of stabilization of axonal MTs that allows persistent growth. More extreme stabilization or destabilization of axonal MTs is likely equally deleterious to axon growth; pharmacological stabilization of MTs might suppress or phenocopy defects in *phr* or *dlk* mutants depending on the context and dosage of the stabilizer.

As the DLK pathway activity emerges as a critical intrinsic determinant of axon regrowth, our findings suggest strategies for overcoming such intrinsic regeneration barriers. For example, inhibition of kinesin-13 could improve regeneration in neurons with less stable MT cytoskeletons, analogous to *C. elegans* mutants with reduced DLK pathway activity. In our genetic studies, axons are chronically exposed to differing levels of enzyme or pathway activity. Future experiments can now address whether acute manipulations of kinesin-13 or of tubulin modifications can have therapeutically relevant effects on regrowth.

Experimental Procedures

C. elegans genetics and molecular biology

C. elegans strains were grown on nematode growth medium agar plates between 15 and 25°C using standard methods. Mutations used in this study are listed in Table S2. We used the following published transgenes: P*mec-7*-GFP(*muIs32*), P*mec-4*-GFP(*zdIs5*); P*unc-25*-GFP(*juIs76*); P*mec-4*-EBP-2::GFP(*juEx2843*) (Chen et al., 2011); P*ccpp-6*-CCPP-6::GFP(*tzEx381*) and P*ttll-9*-TTLL-9::GFP(*tzEx1610*) (Kimura et al., 2010). Standard molecular cloning procedures were used to generate transgenes; see Supplemental Experimental Procedures and Table S1 for details.

EBP-GFP dynamics imaging and analysis

To immobilize worms for imaging without anesthetics we used a suspension of 0.1 μm diameter polystyrene beads (Polysciences 00876-15) on pads composed of 12.5% agarose in M9. EBP-1/2::GFP or GFP::KLP-7 expressing animals were imaged essentially as described (Chen et al., 2011). For live imaging of EBP-2::GFP fluorescence we collected 200 frames of 114 ms exposure each every 230 ms using the Yokogawa CSU-XA1 spinning disc confocal head and a Photometrics Cascade II EMCCD camera (1024 × 1024) controlled by μManager (www.micro-manager.org). Kymographs were generated using Metamorph (Molecular Devices, Sunnyvale, CA) from a region of interest (ROI) placed on the PLM process (Figure 1A,B,D′,D). Typical tracks are displayed as diagonal lines (purple traces in Figure 1B,D). We define appearance and disappearance of EBP-GFP comets as MT rescue/nucleation and catastrophe events (Desai and Mitchison, 1997). We manually traced EBP-GFP tracks on kymographs and calculated their x (growth distance) and y (growth duration) components using Metamorph. Only tracks fully imaged in a movie and longer than 0.57 μm were analyzed. Catastrophe frequency is defined as the number of catastrophe events divided by the total growth time in the kymograph (Stepanova et al., 2010). A small fraction (6%) of comets disappeared and then reappeared in the same position, suggesting a pause in MT growth. Although we include pauses in our calculations of growth duration and velocity, our conclusions are unaltered if pauses are excluded. In most experiments the regrowing PLM axon remained in a single focal plane up to 6 h post axotomy and could be fully imaged. In mutants showing accelerated regrowth (e.g. *klp-7*), the axon often extended into multiple focal planes at 6 h and EBP-2::GFP dynamics could not be reliably imaged.

Antibodies and immunostaining

To analyze tubulin modifications we used the following primary antibodies: rabbit polyclonal anti-Δ2-tubulin (Millipore AB3203, at 1:500 dilution) (Paturle-Lafanechere et al., 1991; Paturle-Lafanechere et al., 1994), rat anti-tyrosinated tubulin (YL1/2 monoclonal, Santa Cruz Biotechnology, 1:100 dilution), and mouse anti-acetylated tubulin (6-11B-1 monoclonal, Sigma, 1:1000 dilution). We visualized alpha tubulins with the DM1A monoclonal (Sigma). Secondary antibodies were from Molecular Probes. Whole-mount immunostaining of larvae and adults followed published methods (Finney and Ruvkun, 1990); fixation steps used 1% paraformaldehyde for 20 min at room temperature. To reduce cuticle crosslinks we incubated fixed samples in 1% β-mercaptoethanol for 15 min, or

overnight for the anti-tyrosinated tubulin staining. We imaged PLM axons in the L4 stage using a Zeiss LSM510 laser scanning confocal microscope. Fluorescence intensities were calculated from 10 μm ROIs along the PLM axon after background subtraction, and expressed as the ratio of red channel (543 or 594 nm excitation) to green (GFP fluorescence, 488 nm excitation). For more details of the immunostaining quantitation methods, see Supplemental Experimental Procedures. Ratios shown in Figure 6 are normalized to wild type controls.

Electron microscopy

Young adult animals were fixed using a high pressure freezing and freeze substitution protocol, as described in detail in Supplemental Experimental Procedures. Most MT counts are from the PLM or ALM process between 100–300 μm from the cell body; approximate position along the process was determined by the presence or absence of AVM and PVM processes in the ventral nerve cord. MT profiles were counted in every 10^{th} section up to a total of 10–30 sections counted, and the average number of profiles per section calculated. No clear trends in MT number were found along processes.

Statistical methods

All statistical analyses used GraphPad Prism. We performed two-way comparisons with Student's t test, the Mann-Whitney test, or Fisher's exact test. Three or more samples were compared with ANOVA or a Kruskall-Wallis test.

Supplementary Material

Refer to Web version on PubMed Central for supplementary material.

Acknowledgments

We thank Thomas Hubert and Lizhen Chen for initial observations on the *ccpp* mutants, Yoshishige Kimura and Mitsutoshi Setou for CCPP reporters, and Dong Yan for DLK-1 reagents. We thank Zilu Wu for assistance with the femtosecond laser. We thank the *C. elegans* Gene Knockout Consortium and the Japanese National Bioresource Project for deletion mutations, and the *Caenorhabditis* Genetics Center for strains; the CGC is supported by the NIH National Center for Research Resources. We thank members of the Jin and Chisholm labs for discussion and suggestions, and Arshad Desai, Shelley Halpain, and María-José Martínez-López for comments on the manuscript. A.G.-R., A.D.C., and Y.J. designed experiments. A.G. performed EM analysis. A.G.-R. performed experiments and analyzed data. A.G.-R., Y.J., and A.D.C. wrote the manuscript. A.G. is an Associate and Y.J. is an Investigator of the Howard Hughes Medical Institute. Supported by NIH R01 NS057317 to A.D.C. and Y.J.

References

Ahmad FJ, Pienkowski TP, Baas PW. Regional differences in microtubule dynamics in the axon. J Neurosci. 1993; 13:856–866. [PubMed: 8426241]

Andrews PD, Ovechkina Y, Morrice N, Wagenbach M, Duncan K, Wordeman L, Swedlow JR. Aurora B regulates MCAK at the mitotic centromere. Dev Cell. 2004; 6:253–268. [PubMed: 14960279]

Baas PW, Ahmad FJ, Pienkowski TP, Brown A, Black MM. Sites of microtubule stabilization for the axon. J Neurosci. 1993; 13:2177–2185. [PubMed: 8478694]

Baas PW, Qiang L. Neuronal microtubules: when the MAP is the roadblock. Trends Cell Biol. 2005; 15:183–187. [PubMed: 15817373]

Bejjani RE, Hammarlund M. Notch signaling inhibits axon regeneration. Neuron. 2012; 73:268–278. [PubMed: 22284182]

Bounoutas A, Kratz J, Emtage L, Ma C, Nguyen KC, Chalfie M. Microtubule depolymerization in *Caenorhabditis elegans* touch receptor neurons reduces gene expression through a p38 MAPK pathway. Proc Natl Acad Sci U S A. 2011; 108:3982–3987. [PubMed: 21368137]

Bradke F, Dotti CG. Differentiated neurons retain the capacity to generate axons from dendrites. Curr Biol. 2000; 10:1467–1470. [PubMed: 11102812]

Bradke F, Fawcett JW, Spira ME. Assembly of a new growth cone after axotomy: the precursor to axon regeneration. Nat Rev Neurosci. 2012; 13:183–193. [PubMed: 22334213]

Cassimeris L. The oncoprotein 18/stathmin family of microtubule destabilizers. Curr Opin Cell Biol. 2002; 14:18–24. [PubMed: 11792540]

Cassimeris L, Pryer NK, Salmon ED. Real-time observations of microtubule dynamic instability in living cells. J Cell Biol. 1988; 107:2223–2231. [PubMed: 3198684]

Chalfie M, Thomson JN. Organization of neuronal microtubules in the nematode *Caenorhabditis elegans*. J Cell Biol. 1979; 82:278–289. [PubMed: 479300]

Chen L, Chisholm AD. Axon regeneration mechanisms: insights from *C. elegans*. Trends Cell Biol. 2011; 21:577–584. [PubMed: 21907582]

Chen L, Wang Z, Ghosh-Roy A, Hubert T, Yan D, O'Rourke S, Bowerman B, Wu Z, Jin Y, Chisholm AD. Axon Regeneration Pathways Identified by Systematic Genetic Screening in *C. elegans*. Neuron. 2011; 71:1043–1057. [PubMed: 21943602]

Dehmelt L, Smart FM, Ozer RS, Halpain S. The role of microtubule-associated protein 2c in the reorganization of microtubules and lamellipodia during neurite initiation. J Neurosci. 2003; 23:9479–9490. [PubMed: 14573527]

Desai A, Mitchison TJ. Microtubule polymerization dynamics. Annu Rev Cell Dev Biol. 1997; 13:83–117. [PubMed: 9442869]

Desai A, Verma S, Mitchison TJ, Walczak CE. Kin I kinesins are microtubule-destabilizing enzymes. Cell. 1999; 96:69–78. [PubMed: 9989498]

Duggan A, Ma C, Chalfie M. Regulation of touch receptor differentiation by the *Caenorhabditis elegans mec-3* and *unc-86* genes. Development. 1998; 125:4107–4119. [PubMed: 9735371]

Ems-McClung SC, Hertzer KM, Zhang X, Miller MW, Walczak CE. The interplay of the N- and C-terminal domains of MCAK control microtubule depolymerization activity and spindle assembly. Mol Biol Cell. 2007; 18:282–294. [PubMed: 17093055]

Erck C, Peris L, Andrieux A, Meissirel C, Gruber AD, Vernet M, Schweitzer A, Saoudi Y, Pointu H, Bosc C, et al. A vital role of tubulin-tyrosine-ligase for neuronal organization. Proc Natl Acad Sci U S A. 2005; 102:7853–7858. [PubMed: 15899979]

Erez H, Spira ME. Local self-assembly mechanisms underlie the differential transformation of the proximal and distal cut axonal ends into functional and aberrant growth cones. J Comp Neurol. 2008; 507:1019–1030. [PubMed: 18092341]

Erturk A, Hellal F, Enes J, Bradke F. Disorganized microtubules underlie the formation of retraction bulbs and the failure of axonal regeneration. J Neurosci. 2007; 27:9169–9180. [PubMed: 17715353]

Fernandez-Gonzalez A, La Spada AR, Treadaway J, Higdon JC, Harris BS, Sidman RL, Morgan JI, Zuo J. Purkinje cell degeneration (pcd) phenotypes caused by mutations in the axotomy-induced gene, Nna1. Science. 2002; 295:1904–1906. [PubMed: 11884758]

Finney M, Ruvkun G. The unc-86 gene product couples cell lineage and cell identity in C. elegans. Cell. 1990; 63:895–905. [PubMed: 2257628]

Gabel CV, Antoine F, Chuang CF, Samuel AD, Chang C. Distinct cellular and molecular mechanisms mediate initial axon development and adult-stage axon regeneration in *C. elegans*. Development. 2008; 135:1129–1136. [PubMed: 18296652]

Ghosh-Roy A, Wu Z, Goncharov A, Jin Y, Chisholm AD. Calcium and cyclic AMP promote axonal regeneration in *Caenorhabditis elegans* and require DLK-1 kinase. J Neurosci. 2010; 30:3175–3183. [PubMed: 20203177]

Gomis-Ruth S, Wierenga CJ, Bradke F. Plasticity of polarization: changing dendrites into axons in neurons integrated in neuronal circuits. Curr Biol. 2008; 18:992–1000. [PubMed: 18595703]

Goodwin PR, Sasaki JM, Juo P. Cyclin-Dependent Kinase 5 Regulates the Polarized Trafficking of Neuropeptide-Containing Dense-Core Vesicles in *Caenorhabditis elegans* Motor Neurons. J Neurosci. 2012; 32:8158–8172. [PubMed: 22699897]

Guillaud L, Bosc C, Fourest-Lieuvin A, Denarier E, Pirollet F, Lafanechere L, Job D. STOP proteins are responsible for the high degree of microtubule stabilization observed in neuronal cells. J Cell Biol. 1998; 142:167–179. [PubMed: 9660871]

Hammarlund M, Nix P, Hauth L, Jorgensen EM, Bastiani M. Axon regeneration requires a conserved MAP kinase pathway. Science. 2009; 323:802–806. [PubMed: 19164707]

Hao L, Thein M, Brust-Mascher I, Civelekoglu-Scholey G, Lu Y, Acar S, Prevo B, Shaham S, Scholey JM. Intraflagellar transport delivers tubulin isotypes to sensory cilium middle and distal segments. Nat Cell Biol. 2011; 13:790–798. [PubMed: 21642982]

Harris A, Morgan JI, Pecot M, Soumare A, Osborne A, Soares HD. Regenerating motor neurons express Nna1, a novel ATP/GTP-binding protein related to zinc carboxypeptidases. Mol Cell Neurosci. 2000; 16:578–596. [PubMed: 11083920]

Helenius J, Brouhard G, Kalaidzidis Y, Diez S, Howard J. The depolymerizing kinesin MCAK uses lattice diffusion to rapidly target microtubule ends. Nature. 2006; 441:115–119. [PubMed: 16672973]

Hellal F, Hurtado A, Ruschel J, Flynn KC, Laskowski CJ, Umlauf M, Kapitein LC, Strikis D, Lemmon V, Bixby J, et al. Microtubule stabilization reduces scarring and causes axon regeneration after spinal cord injury. Science. 2011; 331:928–931. [PubMed: 21273450]

Hendricks M, Jesuthasan S. PHR regulates growth cone pausing at intermediate targets through microtubule disassembly. J Neurosci. 2009; 29:6593–6598. [PubMed: 19458229]

Hirai S, Banba Y, Satake T, Ohno S. Axon formation in neocortical neurons depends on stage-specific regulation of microtubule stability by the dual leucine zipper kinase-c-Jun N-terminal kinase pathway. J Neurosci. 2011; 31:6468–6480. [PubMed: 21525288]

Honnappa S, Gouveia SM, Weisbrich A, Damberger FF, Bhavesh NS, Jawhari H, Grigoriev I, van Rijssel FJ, Buey RM, Lawera A, et al. An EB1-binding motif acts as a microtubule tip localization signal. Cell. 2009; 138:366–376. [PubMed: 19632184]

Howard J, Hyman AA. Microtubule polymerases and depolymerases. Curr Opin Cell Biol. 2007; 19:31–35. [PubMed: 17184986]

Itoh A, Horiuchi M, Bannerman P, Pleasure D, Itoh T. Impaired regenerative response of primary sensory neurons in ZPK/DLK gene-trap mice. Biochem Biophys Res Comm. 2009; 383:258–262. [PubMed: 19358824]

Janke C, Kneussel M. Tubulin post-translational modifications: encoding functions on the neuronal microtubule cytoskeleton. Trends Neurosci. 2010; 33:362–372. [PubMed: 20541813]

Kimura Y, Kurabe N, Ikegami K, Tsutsumi K, Konishi Y, Kaplan OI, Kunitomo H, Iino Y, Blacque OE, Setou M. Identification of tubulin deglutamylase among *Caenorhabditis elegans* and mammalian cytosolic carboxypeptidases (CCPs). J Biol Chem. 2010; 285:22936–22941. [PubMed: 20519502]

Lan W, Zhang X, Kline-Smith SL, Rosasco SE, Barrett-Wilt GA, Shabanowitz J, Hunt DF, Walczak CE, Stukenberg PT. Aurora B phosphorylates centromeric MCAK and regulates its localization and microtubule depolymerization activity. Curr Biol. 2004; 14:273–286. [PubMed: 14972678]

Lewcock JW, Genoud N, Lettieri K, Pfaff SL. The ubiquitin ligase Phr1 regulates axon outgrowth through modulation of microtubule dynamics. Neuron. 2007; 56:604–620. [PubMed: 18031680]

Maney T, Wagenbach M, Wordeman L. Molecular dissection of the microtubule depolymerizing activity of mitotic centromere-associated kinesin. J Biol Chem. 2001; 276:34753–34758. [PubMed: 11466324]

Maniar TA, Kaplan M, Wang GJ, Shen K, Wei L, Shaw JE, Koushika SP, Bargmann CI. UNC-33 (CRMP) and ankyrin organize microtubules and localize kinesin to polarize axon-dendrite sorting. Nat Neurosci. 2012; 15:48–56. [PubMed: 22101643]

Mitchison T, Kirschner M. Dynamic instability of microtubule growth. Nature. 1984; 312:237–242. [PubMed: 6504138]

Montenegro Gouveia S, Leslie K, Kapitein LC, Buey RM, Grigoriev I, Wagenbach M, Smal I, Meijering E, Hoogenraad CC, Wordeman L, et al. In vitro reconstitution of the functional interplay between MCAK and EB3 at microtubule plus ends. Curr Biol. 2010; 20:1717–1722. [PubMed: 20850319]

Nakata K, Abrams B, Grill B, Goncharov A, Huang X, Chisholm AD, Jin Y. Regulation of a DLK-1 and p38 MAP kinase pathway by the ubiquitin ligase RPM-1 is required for presynaptic development. Cell. 2005; 120:407–420. [PubMed: 15707898]

Nix P, Hisamoto N, Matsumoto K, Bastiani M. Axon regeneration requires coordinate activation of p38 and JNK MAPK pathways. Proc Natl Acad Sci U S A. 2011; 108:10738–10743. [PubMed: 21670305]

O'Hagan R, Piasecki BP, Silva M, Phirke P, Nguyen KC, Hall DH, Swoboda P, Barr MM. The Tubulin Deglutamylase CCPP-1 Regulates the Function and Stability of Sensory Cilia in *C. elegans*. Curr Biol. 2011

Paturle-Lafanechere L, Edde B, Denoulet P, Van Dorsselaer A, Mazarguil H, Le Caer JP, Wehland J, Job D. Characterization of a major brain tubulin variant which cannot be tyrosinated. Biochemistry. 1991; 30:10523–10528. [PubMed: 1931974]

Paturle-Lafanechere L, Manier M, Trigault N, Pirollet F, Mazarguil H, Job D. Accumulation of delta 2-tubulin, a major tubulin variant that cannot be tyrosinated, in neuronal tissues and in stable microtubule assemblies. J Cell Sci. 1994; 107(Pt 6):1529–1543. [PubMed: 7962195]

Peris L, Wagenbach M, Lafanechere L, Brocard J, Moore AT, Kozielski F, Job D, Wordeman L, Andrieux A. Motor-dependent microtubule disassembly driven by tubulin tyrosination. J Cell Biol. 2009; 185:1159–1166. [PubMed: 19564401]

Ramon y Cajal, S. Cajal's Degeneration and Regeneration of the Nervous System. Defelipe, J.; Jones, EG., editors; May, RM., translator. New York, NY: Oxford University Press; 1928.

Rogowski K, van Dijk J, Magiera MM, Bosc C, Deloulme JC, Bosson A, Peris L, Gold ND, Lacroix B, Grau MB, et al. A family of protein-deglutamylating enzymes associated with neurodegeneration. Cell. 2010; 143:564–578. [PubMed: 21074048]

Samara C, Rohde CB, Gilleland CL, Norton S, Haggarty SJ, Yanik MF. Large-scale in vivo femtosecond laser neurosurgery screen reveals small-molecule enhancer of regeneration. Proc Natl Acad Sci U S A. 2010; 107:18342–18347. [PubMed: 20937901]

Sengottuvel V, Leibinger M, Pfreimer M, Andreadaki A, Fischer D. Taxol facilitates axon regeneration in the mature CNS. J Neurosci. 2011; 31:2688–2699. [PubMed: 21325537]

Shin JE, Cho Y, Beirowski B, Milbrandt J, Cavalli V, Diantonio A. Dual leucine zipper kinase is required for retrograde injury signaling and axonal regeneration. Neuron. 2012; 74:1015–1022. [PubMed: 22726832]

Srayko M, Kaya A, Stamford J, Hyman AA. Identification and characterization of factors required for microtubule growth and nucleation in the early *C. elegans* embryo. Dev Cell. 2005; 9:223–236. [PubMed: 16054029]

Stepanova T, Slemmer J, Hoogenraad CC, Lansbergen G, Dortland B, De Zeeuw CI, Grosveld F, van Cappellen G, Akhmanova A, Galjart N. Visualization of microtubule growth in cultured neurons via the use of EB3-GFP (end-binding protein 3-green fluorescent protein). J Neurosci. 2003; 23:2655–2664. [PubMed: 12684451]

Stepanova T, Smal I, van Haren J, Akinci U, Liu Z, Miedema M, Limpens R, van Ham M, van der Reijden M, Poot R, et al. History-dependent catastrophes regulate axonal microtubule behavior. Curr Biol. 2010; 20:1023–1028. [PubMed: 20471267]

Suter DM, Schaefer AW, Forscher P. Microtubule dynamics are necessary for SRC family kinase-dependent growth cone steering. Curr Biol. 2004; 14:1194–1199. [PubMed: 15242617]

Usher LC, Johnstone A, Erturk A, Hu Y, Strikis D, Wanner IB, Moorman S, Lee JW, Min J, Ha HH, et al. A chemical screen identifies novel compounds that overcome glial-mediated inhibition of neuronal regeneration. J Neurosci. 2010; 30:4693–4706. [PubMed: 20357120]

Vale RD, Fletterick RJ. The design plan of kinesin motors. Annu Rev Cell Dev Biol. 1997; 13:745–777. [PubMed: 9442886]

Witte H, Bradke F. The role of the cytoskeleton during neuronal polarization. Curr Opin Neurobiol. 2008; 18:479–487. [PubMed: 18929658]

Witte H, Neukirchen D, Bradke F. Microtubule stabilization specifies initial neuronal polarization. J Cell Biol. 2008; 180:619–632. [PubMed: 18268107]

Wu Z, Ghosh-Roy A, Yanik MF, Zhang JZ, Jin Y, Chisholm AD. *Caenorhabditis elegans* neuronal regeneration is influenced by life stage, ephrin signaling, and synaptic branching. Proc Natl Acad Sci U S A. 2007; 104:15132–15137. [PubMed: 17848506]

Xiong X, Wang X, Ewanek R, Bhat P, Diantonio A, Collins CA. Protein turnover of the Wallenda/DLK kinase regulates a retrograde response to axonal injury. J Cell Biol. 2010; 191:211–223. [PubMed: 20921142]

Yan D, Wu Z, Chisholm AD, Jin Y. The DLK-1 kinase promotes mRNA stability and local translation in *C. elegans* synapses and axon regeneration. Cell. 2009; 138:1005–1018. [PubMed: 19737525]

Yu W, Ahmad FJ, Baas PW. Microtubule fragmentation and partitioning in the axon during collateral branch formation. J Neurosci. 1994; 14:5872–5884. [PubMed: 7931550]

Zhang X, Lan W, Ems-McClung SC, Stukenberg PT, Walczak CE. Aurora B phosphorylates multiple sites on mitotic centromere-associated kinesin to spatially and temporally regulate its function. Mol Biol Cell. 2007; 18:3264–3276. [PubMed: 17567953]

Highlights

- Axon injury triggers a two-phase process of microtubule (MT) growth upregulation
- The depolymerizing kinesin-13 KLP-7 is locally downregulated at the axon stump
- Tubulin post translational modifications regulate axon regeneration
- The DLK-1 pathway regulates both axonal kinesin-13 and tubulin modifications

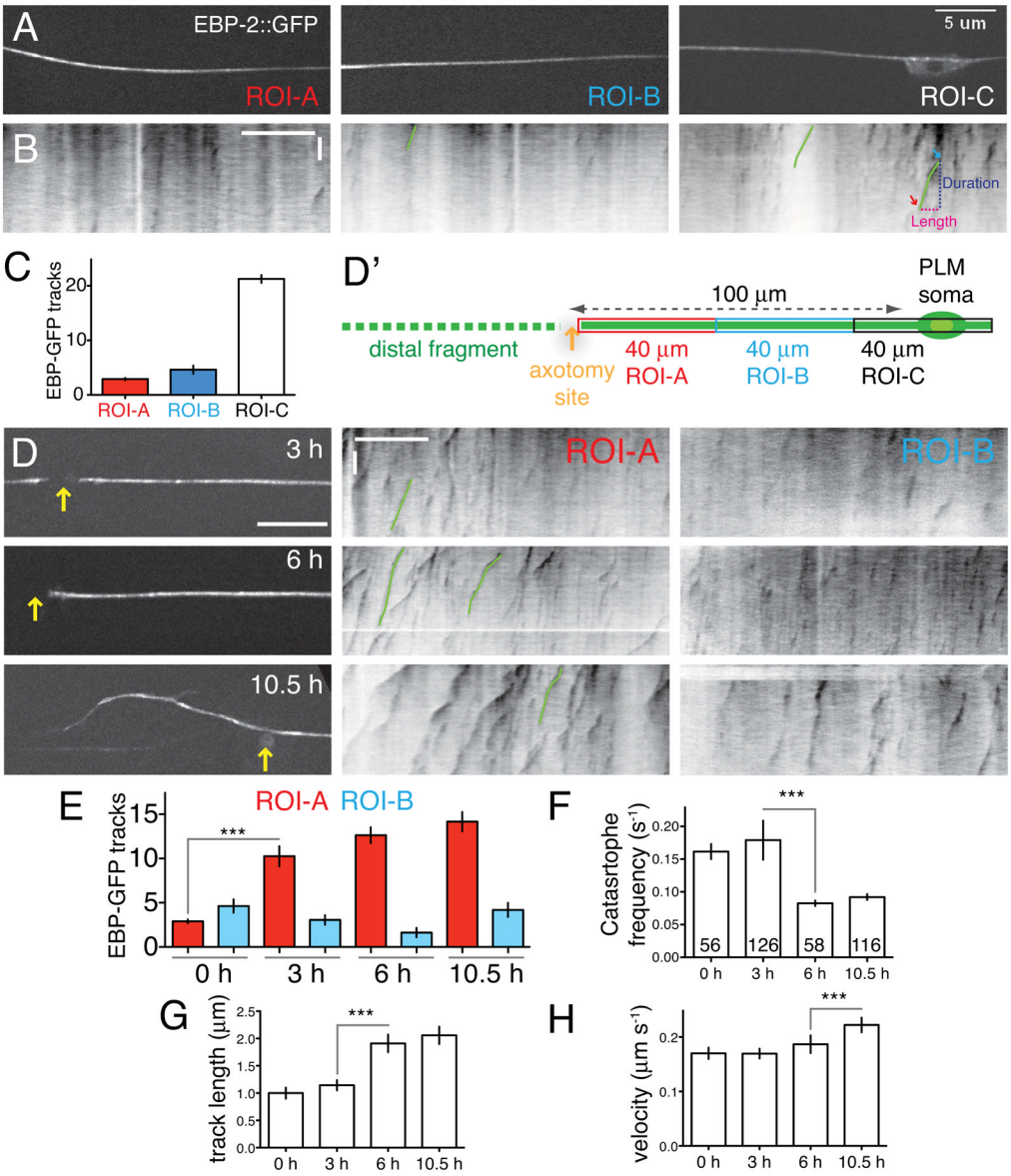

Figure 1. Axon injury triggers MT reorganization in two stages

(A) EBP-2::GFP dynamics in mature PLM axons in L4 stage or young adults. Axons were divided into three 40 µm long regions of interest (ROI-A,B,C) and EBP-2::GFP (*juEx2843*) imaged using spinning disc confocal microscopy. (B) Representative kymographs (inverted grayscale) of EBP-2::GFP tracks prior to injury; see also Supplemental Movies 1,2. Green lines in kymographs delineate representative EBP-2::GFP tracks; blue and red arrows indicate putative 'rescue' and 'catastrophe' events. In all kymographs the length (x axis) and time (y axis) scales are 10 µm and 10 s. (C) In the steady state, EBP-GFP comets are largely confined to the PLM soma (ROI-C) and rare in the axon shaft (ROI-A,B); n = 11 axons. (D) Single frames of EBP-2::GFP after injury (yellow arrows indicate positions of axotomy); kymographs of EBP-2::GFP movement in ROI-A and B. (D′) Location of ROIs relative to site of axotomy. (E) Local upregulation of numbers of EBP-2::GFP tracks in kymographs from ROI-A (red) and ROI-B (blue) before and after axotomy; n ≥ 9 axons per condition. (F) Increase in MT growth from 3 to 6 h. (F–H) Catastrophe frequency (inverse of average growth duration), growth length (µm), and velocity (µm s^{-1}) of EBP-2::GFP tracks in

kymographs of ROI-A, before and after axotomy. Error bars depict mean ± SEM. Numbers on the bars indicate number of tracks in F–H. Statistics, Kruskal-Wallis test; *, $P < 0.05$; ***, $P < 0.001$. See also Figure S1 and Table S1.

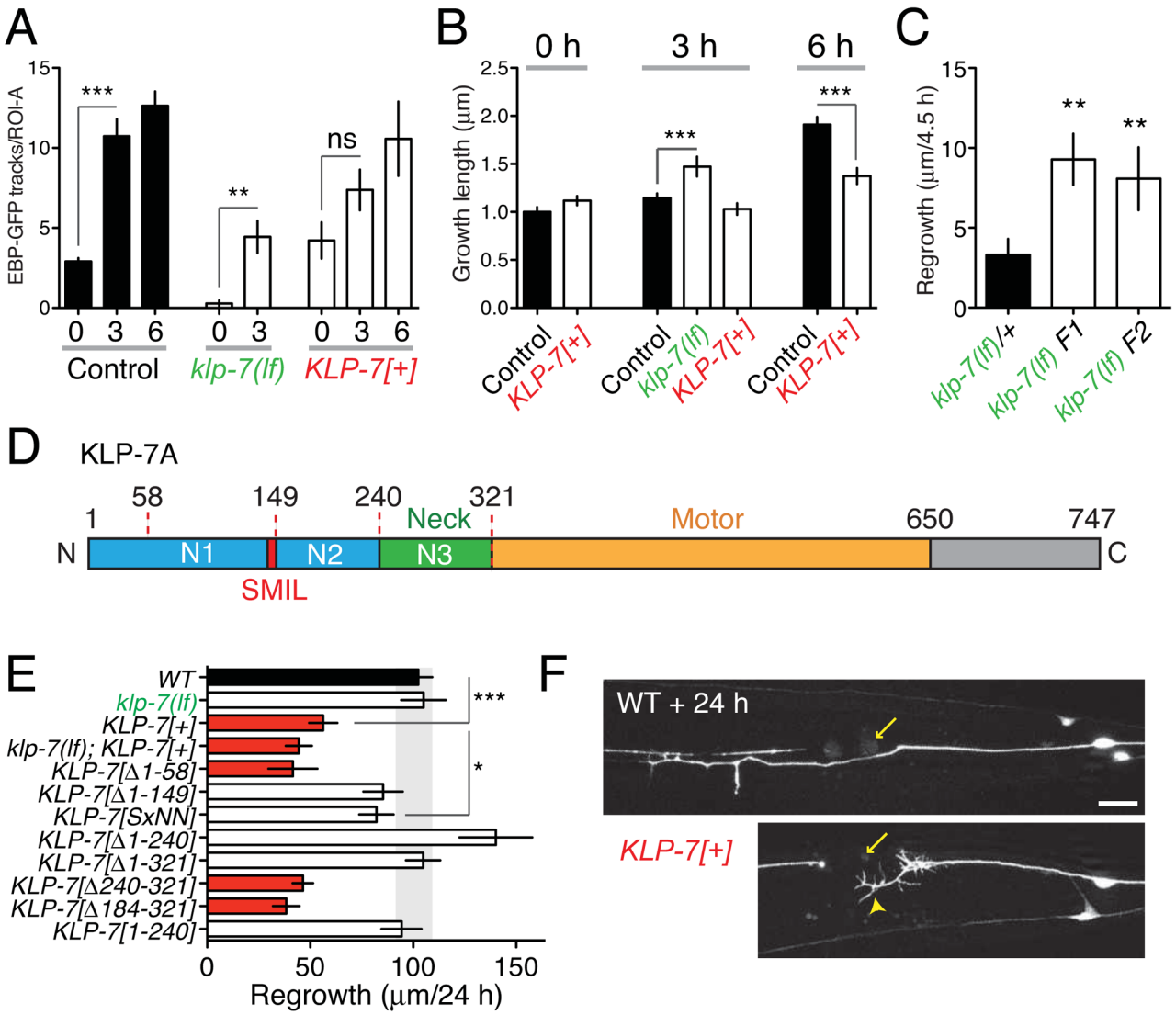

Figure 2. The MT-depolymerizing kinesin KLP-7 negatively regulates microtubule upregulation and inhibits regeneration

(A) KLP-7 negatively regulates the upregulation of growing MTs after axotomy. *klp-7(lf)* mutants have few growing MTs in the steady state, and upregulate the number of growing MTs over 10-fold after axotomy. KLP-7 overexpressors (*juEx3842*) have normal steady state growing MTs and do not significantly upregulate (1.7-fold) growing MTs. n > 7 axons per genotype. As *klp-7(lf)* mutants display almost no growing MTs in the steady state we do not report data for this genotype at 0 h. Statistics, Mann-Whitney test. (B) KLP-7 inhibits the increase in persistent EBP-GFP growth from 3–6 h; n ≥ 30 tracks per condition. Statistics, ANOVA. (C) *klp-7(lf)* mutants display increased regrowth at 4.5 h post axotomy; F1 and F2 denote animals in the F_1 or F_2 generation from *klp-7(lf)/+* heterozygous parents. (D) KLP-7 protein domains; N1, N2, and N3 denote N-terminal regions used in designing mutations (see Figure 5). The SxIL motif begins at residue S148. (E) KLP-7 overexpression inhibits regrowth, and requires the N-terminus and SxIL motif. Background, P*mec-7*-GFP(*muIs32*); n, number of axons ≥ 8 per genotype. ANOVA and Bonferroni post test. (F) Abnormal growth cone morphology 24 h after axotomy in KLP-7-overexpressing animals. Error bars depict mean ± SEM. See also Figure S2.

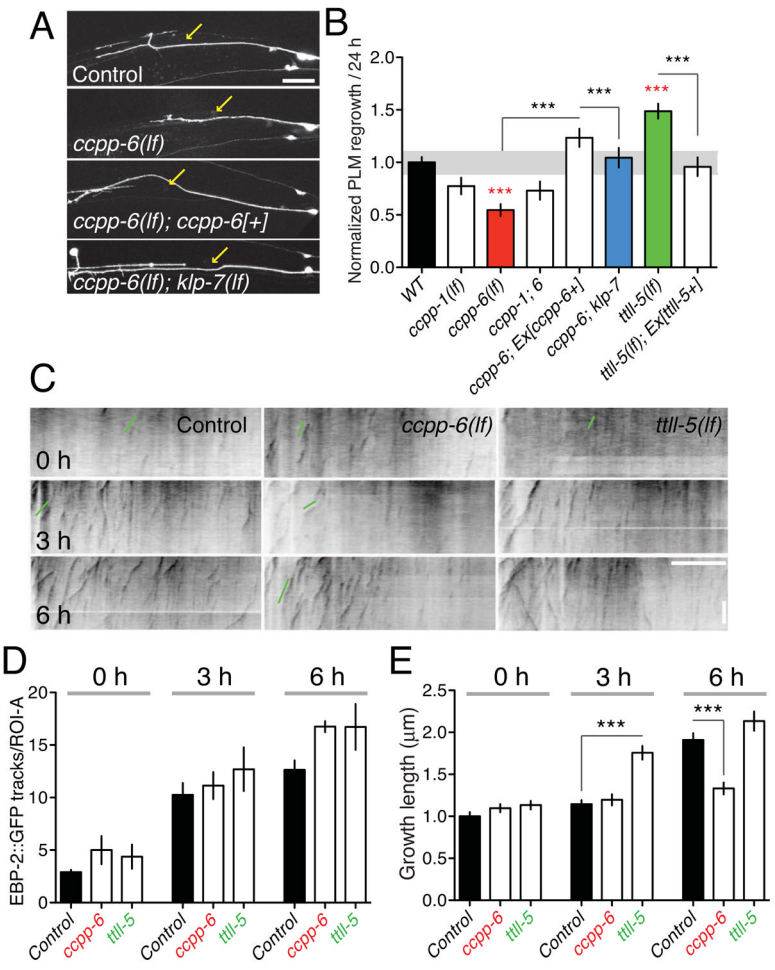

Figure 3. Tubulin post-translational modification enzymes regulate the second phase of microtubule stabilization

(A,B) CCPP-6 is required cell autonomously for PLM regrowth; *ccpp-6(lf)* phenotypes are suppressed by *klp-7(lf)*. Confocal images of regrowing PLM axons from control (*muIs32*), *ccpp-6(lf)*, *ccpp-6(lf); juEx3889*(P*mec-4*-CCPP-6), and *ccpp-6(lf); klp-7(lf)*, 24 h after axotomy. (B) Regrowth in tubulin post-translational modification mutants, rescue, and suppression of *ccpp-6(lf)* by *klp-7(lf)*; n = 10–30 axons per genotype; Regrowth normalized to WT, shaded band indicates 90% CI of WT; ANOVA, Bonferroni post test. (C) EBP-2::GFP dynamics in ROI-A in wild type, *ccpp-6*, and *ttll-5* mutants after axotomy. (D) Neither *ccpp-6(lf)* nor *ttll-5(lf)* affect steady-state EBP-2::GFP tracks or upregulation at 3 h. (E) *ccpp-6* mutants fail to transition to persistent EBP-2::GFP track growth at 6 h; *ttll-5* mutants display a premature transition to persistent growth at 3 h; n ≥ 25 per condition for D,E. Error bars depict mean ± SEM. Statistics, t test. See also Figure S3.

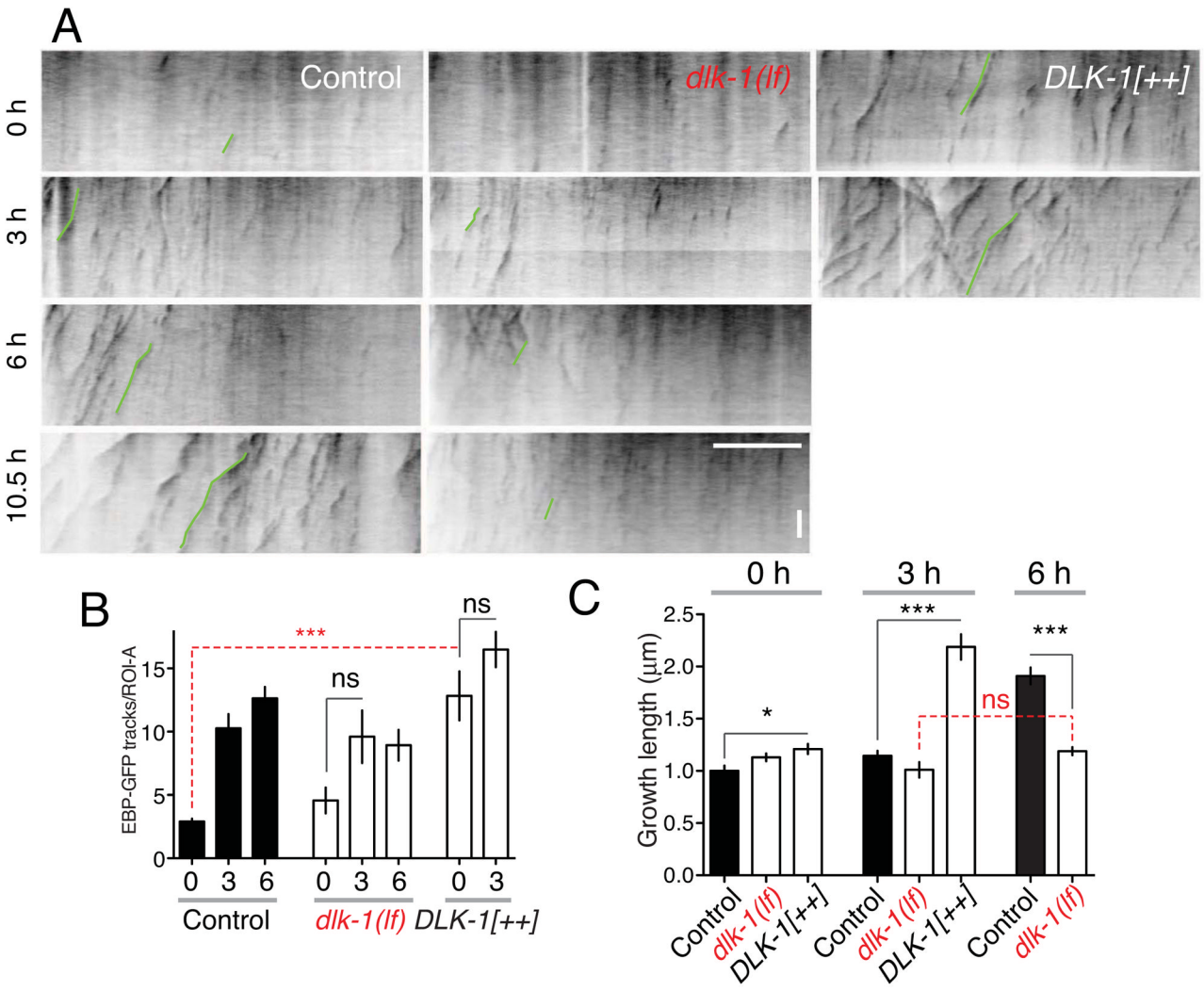

Figure 4. The DLK-1 pathway is necessary and sufficient to promote persistent microtubule growth

(A) Kymographs of EBP-2::GFP in ROI-A of PLM axon in control, *dlk-1(ju476)* mutants, and DLK-1 overexpressing backgrounds, P*rgef-1-DLK-1[+](juEx3526)*. (B) In *dlk-1(lf)* mutants MT upregulation at 3 h is reduced compared to wild type. DLK-1 overexpression causes a large increase in EBP-GFP tracks in the absence of injury; injury does not further increase the number of EBP-GFP tracks. n ≥ 8 axons per genotype. (C). Persistent MT growth at 6 h is completely blocked in *dlk-1(lf)*, whereas DLK-1 overexpression causes increased EBP-GFP track length before and after injury. n (number of tracks) ≥ 45 per condition. Error bars depict mean ± SEM. Statistics, Kruskall-Wallis test, Dunn post test. See also Figure S4.

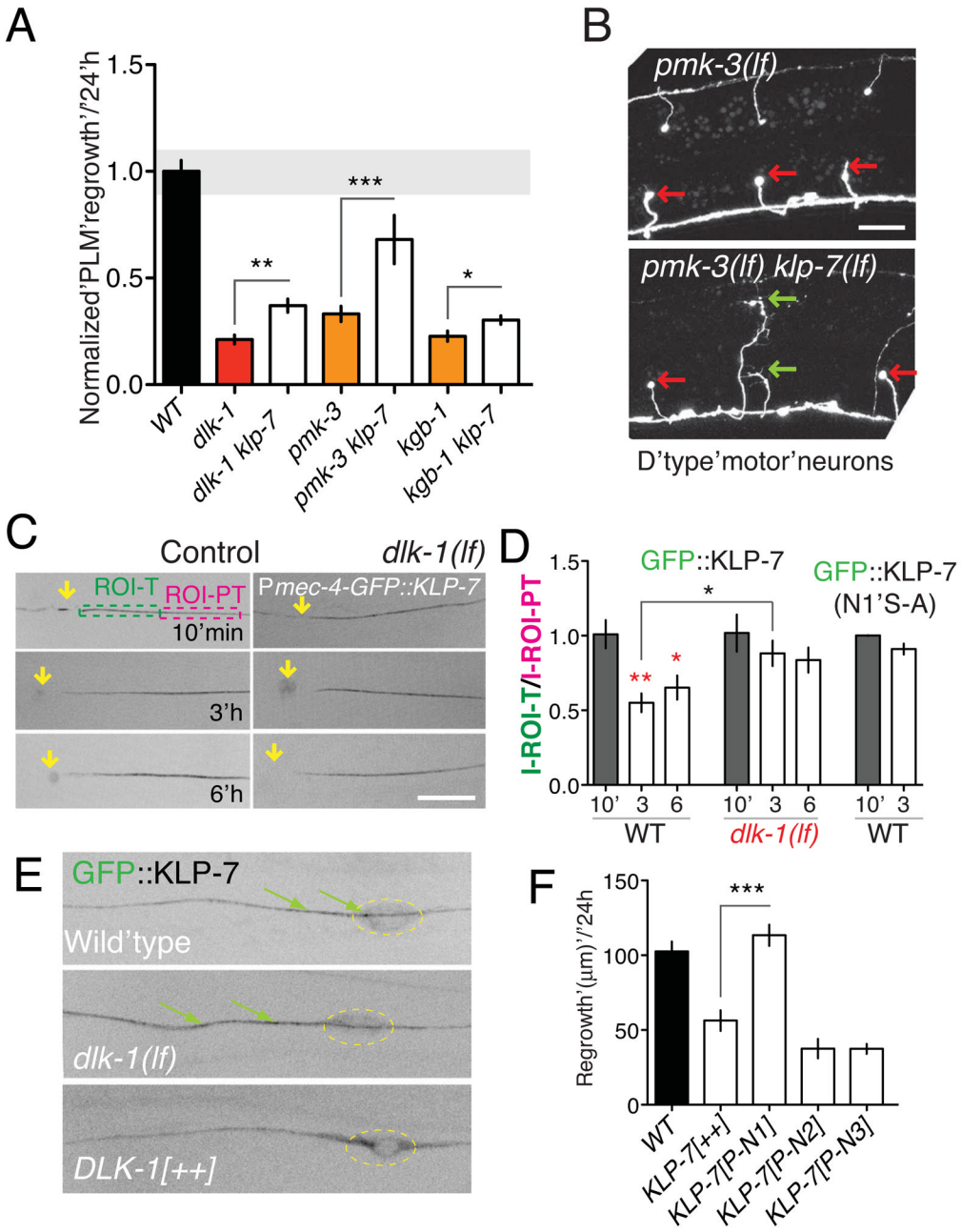

Figure 5. The DLK-1 pathway locally downregulates KLP-7 after axotomy

(A) *klp-7(lf)* suppresses PLM regrowth defects in *dlk-1* (MAPKKK), *pmk-3* (MAPK), and *kgb-1* (MAPK) mutants; normalized regrowth as in Figure 3B. (B) *klp-7(lf)* suppresses motor neuron regrowth defects of *pmk-3*; representative images 24 h post axotomy of D neuron commissures (*juIs76* marker). After axotomy, *pmk-3* mutant D neurons do not regrow, forming retraction bulbs (red arrows); 0/52 D neurons displayed growth cones at 24 h. In *pmk-3 klp-7*, 16/45 D neurons formed growth cone like structures (green arrows). (C) Frames from time-lapse movies of GFP::KLP-7 (*juEx4219*) in PLM at 10 min, 3 h, and 6 h after axotomy, in control and *dlk-1(lf)* backgrounds. At 3 and 6 h the intensity of GFP::KLP-7 was reduced near the injured axon tip, as measured in ROIs (ROI-T and ROI-PT) spanning the first 30 µm of the axon tip. (D) Ratio of GFP::KLP-7 or GFP::KLP-7(N1

S-A) fluorescence intensity in ROI-T vs. ROI-PT at 10 min, 3 h or 6 h post axotomy, in wild type or *dlk-1(lf)*; n ≥ 7 per condition. (E) Confocal sections of the PLM axon and cell body of animals expressing GFP::KLP-7(*juEx4219*) in wild type, *dlk-1(lf)* and *DLK-1[++] (juEx3526)* backgrounds. In DLK-1 overexpressing neurons GFP::KLP-7 is excluded from the axon. Scale, 10 μm. (F) Putative phosphorylation sites in the N1 region are critical for the growth-inhibiting role of KLP-7. PLM regrowth measured 24 h after axotomy of control and transgenic animals expressing phosphomimetic mutants of KLP-7. Error bars depict mean ± SEM. Statistics, ANOVA: *, P < 0.05; **, P < 0.01; ***, P, 0.001. See also Figure S5.

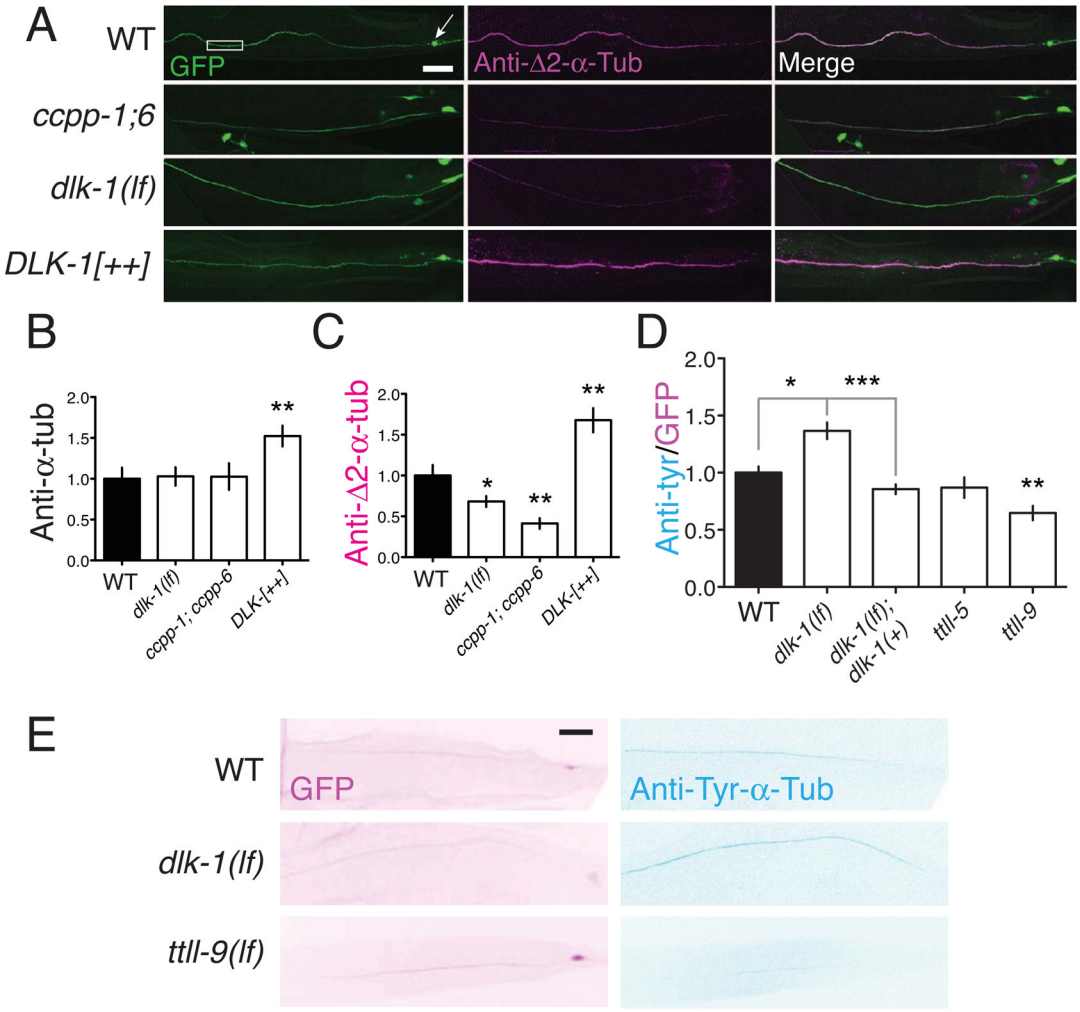

Figure 6. The DLK pathway regulates tubulin post-translational modifications in axonal MTs

(A) CCPPs and DLK-1 promote formation of stable Δ2-modified microtubules. Anti-Δ2-tubulin immunostaining in PLM axons is significantly decreased in *ccpp* double mutants and in *dlk-1(lf)* mutants, and increased in animals overexpressing DLK-1. Confocal images; touch neuron axons are labeled with GFP [*muIs32*]. Scale, 10 μm. (B,C,D) Quantitation of anti-pan-α-tubulin, anti-Δ2-tubulin, and anti-Tyr-α-tubulin immunostaining, normalized to WT. Statistics, t test. (E) Confocal projections of GFP and anti-Tyr-α-tubulin staining in *muIs32* background (inverted color scale, D). Error bars depict mean ± SEM. See also Figure S6 and Table S2.

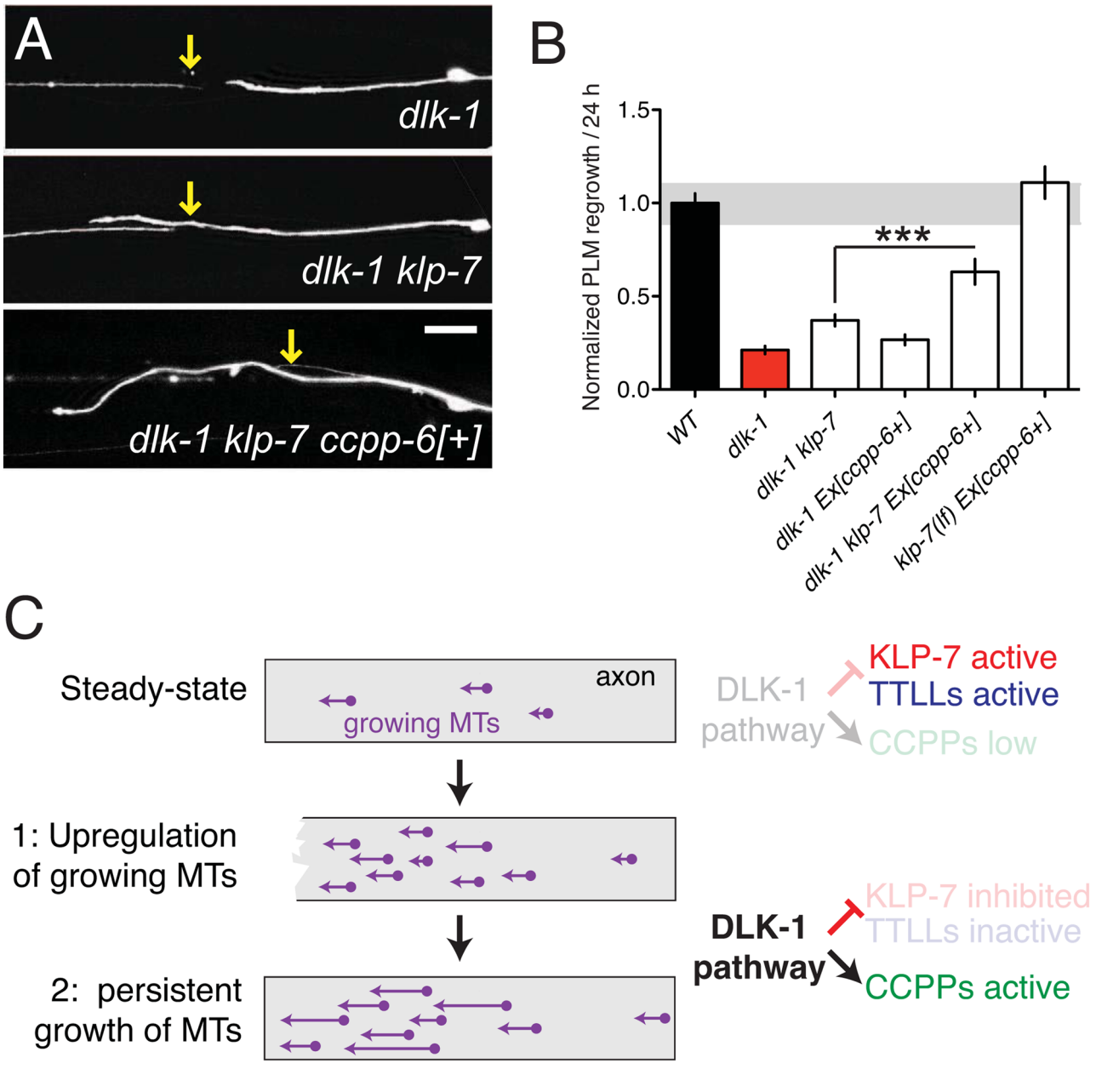

Figure 7. Combined downregulation of KLP-7 and upregulation of CCPPs can overcome the requirement for the DLK pathway in regrowth

(A,B) The *dlk-1* regeneration block is not suppressed by overexpression of CCPP enzymes except in the absence of *klp-7*. Confocal images of PLM axons and quantitation of 24 h regrowth. Scales, 10 μm. (C) Model of the two phases of axon MT dynamics and proposed regulatory roles for the DLK pathway. Error bars depict mean ± SEM. See also Figure S7.